Fingering in a driven Hele-Shaw cell

Steven N. Rauseo*
Physics Department, Wheaton College, 501 College Avenue, Wheaton, Illinois 60187
(Received 26 May 2000; revised manuscript received 14 August 2000)

A modified Hele-Shaw cell in which the plate gap can be modulated in time was constructed. Highly nonlinear fingers on the interface between air and water in the cell were observed as the plate gap was driven at a variety of frequencies, but typically near 60 Hz. Modified equations to describe the flow in a periodically driven cell were derived and the linear stability analysis of waves on a circular fluid-fluid interface was performed.

PACS number(s): 47.20.Ma, 47.54.+r, 05.45.Xt

I. INTRODUCTION

The Hele-Shaw cell (two parallel plates separated by a small gap through which fluids flow) has been used extensively to model fluid flow in highly resistive porous media, as well as a device for the study of simple pattern-forming systems [1,2]. Hele-Shaw cells are used to model flow in porous media since in both systems the fluid velocity is simply proportional to the gradient of the pressure. Darcy's law expresses this as $\mathbf{v}=-M\nabla p$. In the Hele-Shaw cell, the velocity is averaged over the spatial dimension perpendicular to the plates, and $M=b^2/12\mu$, where b is the gap between the plates and μ is the fluid viscosity.

The unstable interface between two fluids of differing viscosity form one of the simplest pattern-forming systems. Since the velocity is proportional to the gradient of the pressure, and for $\nabla\cdot\mathbf{v}=0$ when ρ is constant in time, the pressure obeys Laplace's equation $\nabla^2 p=0$. Thus, the unstable growth of a driven interface is an example of Laplacian growth, a class of problems that includes dielectric breakdown, diffusion-limited aggregation (DLA), and the colonial growth of certain organisms. Multiple variations have been studied extensively: immiscible, miscible, and non-Newtonian fluids, rectangular, and circular geometries, as well as cells with various symmetries etched on one or both faces [3–6].

A modification of the Hele-Shaw cell was designed and built that allows the gap to be varied in time. The motivation was to introduce a method in which the interface could be driven periodically. For the parameter values where the flow can still be viewed as two dimensional, the plate variation has the effect of drawing fluid out (a sink), or putting fluid in (a source), at each point in the plane. Thus the pressure is no longer governed by Laplace's equation, but by Poisson's equation.

Equations for the fluid velocity in the *x-y* plane are derived in this paper, and using these, the linear stability analysis for an initially circular interface between two fluids in the cell is performed. Preliminary experimental results are reported, especially the behavior of the fingers which form on the driven interface.

*Email address: steven.n.rauseo@wheaton.edu

II. EXPERIMENTAL APPARATUS

The essential portion of the modified Hele-Shaw cell is a 7.62 cm (3 in) radius circular quartz plate below and a 6.35 cm (2.5 in.) radius stainless-steel upper plate. The lower quartz plate is a 1/4 wavelength optical flat and is thus flat to under 0.2 μm. The upper plate was machined to be flat to about 15 μm, and has 3 μm deep random scratches from the finishing process. For the experiments reported here, the gap between the plates was in the range 230–420 μm. The upper plate is supported via a 1/4 in. thick aluminum plate that is itself attached to a Terfenol actuator [8], which allows the plate to be moved up to 80 μm up or down at frequencies up to 2 kHz. The lower plate is supported in a stainless-steel base, with a 6.35 cm radius hole that allows the fluids in the cell to be observed from below (Fig. 1).

The cell was typically driven near 60 Hz, to keep it far from any mechanical resonances in the apparatus and to allow synchronization with a videocamera's field rate of 59.93 Hz. Other multiples or factors of 60 Hz were also used (e.g., 180 or 15 Hz). The fluids used were most typically water and air. The water had 3 g/liter of fluorescein dye added and the apparatus was illuminated from below with ultraviolet light.

III. EQUATION MODIFICATION

Both the continuity equation and Darcy's law must be modified for this new cell. One wishes to reduce the problem to two spatial dimensions by averaging all variables over the

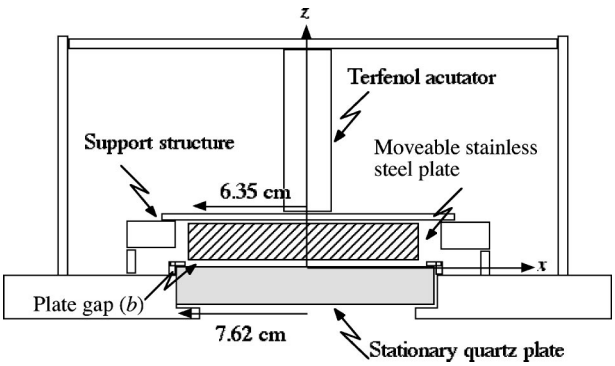

FIG. 1. Cut away side view of the cell. The inner fluid is confined to the space between the plates, while the outer fluid is between and surrounds the plates. The axes defined in the text are shown. The fluids are illuminated and viewed from below.

direction perpendicular to the plates. (Call this the z direction.) Define a two-dimensional velocity $\mathbf{u}$ to be the x and y components of the z-averaged velocity, e.g., $u_x(x,y) = (1/b)\int_0^b v_x(x,y,z)dz$, where the origin is set at the center of the cell in the x and y directions and at the bottom plate in the z direction.

Begin with the continuity equation $\rho(\nabla\cdot\mathbf{v})+(\partial\rho/\partial t) = 0$. In the case where the fluid density ρ is constant with time, one is left with $(\partial/\partial x)v_x+(\partial/\partial y)v_y+(\partial/\partial z)v_z=0$. Averaging the first two terms over the z direction simply gives the divergence of the z-averaged velocity $\mathbf{u}$. The third term is then $(1/b)\int_0^b[(\partial/\partial z)v_z]dz=v_z(x,y,z=b) - v_z(x,y,z=0)$.

The z component of the velocity must be zero at the lower, stationary plate, but it must match the motion of the top plate, so it is $(\partial/\partial t)b(t)$. The new continuity equation is therefore

$$\nabla\cdot\mathbf{u}=-\frac{1}{b(t)}\frac{\partial}{\partial t}b(t). \tag{1}$$

To derive the new equation of motion for the fluids in the cell, start with the Navier-Stokes equation

$$\rho\left(\frac{\partial}{\partial t}\mathbf{v}+(\mathbf{v}\cdot\nabla)\mathbf{v}\right)=-\nabla p+\mu\nabla^2\mathbf{v}. \tag{2}$$

Most of the assumptions made in the derivation of Darcy's law for flow in a Hele-Shaw cell can be made: the Laplacian of the velocity is the greatest in the z direction and the term $\rho(\mathbf{v}\cdot\nabla)\mathbf{v}$ can be ignored relative to the viscosity term. If, however, the frequency at which the upper plate is moved is sufficiently high the $\rho(\partial/\partial t)\mathbf{v}$ term cannot be ignored. (The amplitude of the motion must not be so large as to produce high velocities and thus require returning to the full Navier-Stokes equation.) Finally, as in the ordinary Hele-Shaw cell, we assume that the dependence of the x and y components of the velocity on z is simply parabolic. For instance, take $v_x(z)=az(z-b)$. Integrating over z yields $u_x=(1/b)\int_0^b v_x dz=-ab^2/6$, or $a=-6u_x/b^2$. Combining these assumptions yields

$$\rho\frac{\partial}{\partial t}v_x=-\nabla p+2\mu a \tag{3}$$

and a similar equation for the y component of $\mathbf{v}$. Integrating Eq. (3) over z from 0 to b yields the new equation for $\mathbf{u}$ in the x-y plane

$$\rho\left(\frac{\partial}{\partial t}\mathbf{u}\right)+\rho\left(\frac{1}{b(t)}\frac{\partial}{\partial t}b(t)\right)\mathbf{u}+\frac{12\mu}{b(t)^2}\mathbf{u}=-\nabla p, \tag{4}$$

where the gradient is now taken only in the x-y plane. The term $\rho([1/b(t)](\partial/\partial t)b(t))\mathbf{u}$ arises from bringing the integration over z inside the time derivative, since b is an explicit function of time.

IV. LINEAR STABILITY ANALYSIS

For convenience define an operator

$$\mathcal{D}_t=\left(\rho\frac{\partial}{\partial t}+\frac{\rho}{b(t)}\frac{\partial b(t)}{\partial t}+\frac{12\mu}{b(t)^2}\right)$$

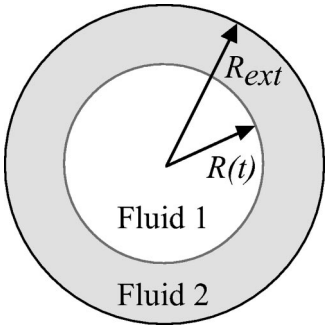

FIG. 2. View of cell from below defining R_{ext} and $R(t)$.

which is an operator in time only. Then the equation of motion [Eq. (4)] can be written as

$$\mathcal{D}_t\mathbf{u}=-\nabla p. \tag{5}$$

Taking the divergence of both sides and combining with the continuity equation [Eq. (1)] yields the Poisson equation for the pressure

$$\nabla^2 p=-\mathcal{D}_t\nabla\cdot\mathbf{u}=\mathcal{D}_t\left(\frac{1}{b(t)}\frac{\partial b(t)}{\partial t}\right). \tag{6}$$

Now consider the problem of an initially circular interface between two fluids placed symmetrically in a cell of external radius R_{ext} (Fig. 2). The pressure has a circularly symmetric solution

$$p(r)=\frac{1}{4}\mathcal{D}_t\left(\frac{1}{b(t)}\frac{\partial b(t)}{\partial t}\right)r^2+C\ln(r)+p_0.$$

Note that the constant of integration C does not depend on r, but in general is a function of time and the position of the interface R. The continuity equation yields a solution for the velocity

$$u_r=-\frac{1}{2}\left(\frac{1}{b(t)}\frac{\partial b(t)}{\partial t}\right)r+\frac{C'}{r},$$

with C and C' related by $C=\mathcal{D}_tC'$. If both fluids are incompressible then continuity at the origin requires $C=C'=0$. If the inner fluid is compressible, these terms survive in the equations for the outer fluid.

Consider first perturbations of the interface in the case of two incompressible fluids. Following Paterson [7], introduce the expression for a perturbation of the interface in the form $dr=ah(t)e^{in\theta}$, $n=1,2,3,\ldots$.

Such a perturbation will result in a change in the pressure such that

$$p(r)=\frac{1}{4}\mathcal{D}_t\left(\frac{1}{b(t)}\frac{\partial b(t)}{\partial t}\right)r^2+(-1)^jA\left(\frac{r^n}{R^n}\right)^{(-1)^{j-1}}e^{in\theta},$$

where $j=1$ for the inner fluid and 2 for the outer. Requiring continuity in the velocity at the interface (to first order in a) at $r=R(t)$ yields

$$A=-\frac{1}{2}\frac{R(t)\left[24\mu\left(\frac{\partial}{\partial t}h(t)\right)+\rho b(t)\left(\frac{\partial}{\partial t}b(t)\right)\left(\frac{\partial}{\partial t}h(t)\right)+2\rho b(t)\left(\frac{\partial^2}{\partial t^2}h(t)\right)\right]}{nb(t)^2}a.$$

The pressure drop across the interface is given by the surface tension σ times the curvature of the interface κ, so

$$p_1-p_2=\sigma\left(\frac{2}{b}+\frac{1}{R}-\frac{dr+\frac{d^2}{d\theta^2}dr}{R^2}\right).$$

To first order in a, these equations yield a differential equation for $h(t)$,

$$\frac{d^2}{dt^2}h(t)+\frac{1}{2b(t)^2}\left(\frac{24\mu_1+\mu_2}{\rho_1+\rho_2}+b(t)\frac{d}{dt}b(t)\right)\left(\frac{d}{dt}h(t)\right)+\frac{1}{2b(t)^3(\rho_1+\rho_2)}\left((\rho_2-\rho_1)b(t)^2\frac{d^2}{dt^2}b(t)+12(\mu_2-\mu_1)n\frac{d}{dt}b(t)+2\frac{\sigma}{R(t)^3}(n^3-n)b(t)^3\right)h(t)=0.$$

When the volume of the inner fluid must be conserved, $R(t)=R(0)\sqrt{b(0)/b(t)}$. The net result is a damped oscillator equation for $h(t)$ in which the damping term (the coefficient of dh/dt) and the restoring term (the coefficient of h) are both functions of time. While such an equation cannot in general be solved in closed form, it is clear that the perturbation will grow rapidly whenever the ''damping'' or ''restoring'' terms become negative.

Numeric solutions of the equations for two simple immiscible fluids (paraffin oil as the inner fluid, water as the outer), yield predictions for the drive strength necessary to see the instability. Using parameters typical for this apparatus [$b_0=290\,\mu$m, $f=60$ Hz, $R(0)=0.031$ m], the calculations predict that the interface will not become unstable until $b_1=39\,\mu$m at $n=105$.

The case of the inner fluid being compressible is more complex, not simply because the $\ln(r)$ term cannot be ignored in the unperturbed solution for the pressure, but also because the coefficient C' in the velocity is itself governed by a differential equation.

The pressure of the inner fluid is assumed to be uniform throughout. Since the gap is set typically quite small (less than 0.3 mm) and the surrounding materials have high thermal conductivity, the compression can safely be viewed as isothermal. Thus, for the circularly symmetric solution, $p_1(t)=p_1(0)R(0)^2b(0)/[b(t)R(t)^2]$. Assuming that the cell is not moving before $t=0$, $p_0=p_1(0)=p_{ext}+\sigma[(2/b_0)+(1/R_0)]$, where $R_0=R(0)$, $b_0=b(0)$, and p_{ext} is the pressure just outside the cell (and is assumed to be constant).

The outer fluid has the initial pressure

$$p(r)=\frac{1}{4}\mathcal{D}_t\left(\frac{1}{b(t)}\frac{\partial b(t)}{\partial t}\right)(r^2-R_{ext}^2)+C\ln\left(\frac{r}{R_{ext}}\right)+p_{ext},$$

where R_{ext} is the outer radius of the cell. The constant C is calculated by integrating the gradient of the pressure from $r=R_{ext}$ to $r=R_0$ and using

$$p_1(t)=\left[p_2(r,t)+\sigma\left(\frac{2}{b}+\frac{1}{r}\right)\Big|_{r=R}\right],$$

at the unperturbed interface.

Following the same procedure as before, the interface is perturbed by dr and the continuity of velocity and pressure at the interface are invoked. The end result is a differential equation for $h(t)$,

$$\frac{d^2}{dt^2}h(t)+2\gamma(t)\frac{d}{dt}h(t)+\Omega^2(t)h(t)=0$$

where

$$\gamma(t)=\frac{1}{4b(t)^2}\left(b(t)\frac{b}{dt}b(t)+24\frac{\mu_2}{\rho_2}\right)$$

and

$$\Omega^2(t)=\left(\frac{(n^2-1)\sigma}{R^3\rho}+\frac{6\mu}{b^3\rho}\frac{d}{dt}b+\frac{1}{2b}\frac{d^2}{dt^2}b+\frac{1}{\ln\left(\frac{R}{R_{ext}}\right)}\left(\frac{(2R_0+b_0)R_0\sigma+(R^2b-R_0^2b_0)P_{ext}}{bR^4\rho}-\frac{3\mu}{b^3\rho}\frac{d}{dt}b-\frac{1}{4}\frac{d^2}{dt^2}b\right)\right)n,$$

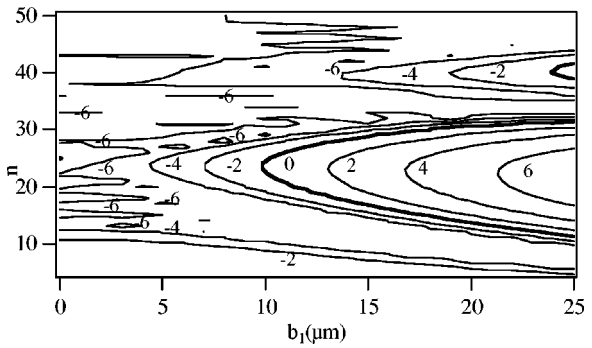

FIG. 3. Calculated growth exponent for a sinusoidal perturbation after ten periods of the plate drive as a function of the drive amplitude b_1 and the number of wavelengths around the interface n. The average plate gap $b_0 = 290\ \mu$m and the frequency of the drive is $f = 60$ Hz. The growth exponent first becomes positive (indicating unstable growth) for $n = 23$ when $b_1 = 9.6\ \mu$m. For these parameters the actual interface first sees waves at $b_1 = 25\ \mu$m and the fingers erupt at $b_1 = 30\ \mu$m.

where R and b are both functions of time only. A further complication in this case is that the position of the interface is not simply related to the plate gap, but that together with the constant C' it is governed by a set of coupled differential equations: $\mathcal{D}_t C' = C$ and $d/dtR = u_r(r,t)|_{r=R} = (1/bd/dtb)R + C'/R$. Shown in Fig. 3 is the calculated growth of perturbation assuming sinusoidal driving of the plates $b(t) = b_0 + b_1 \sin(\omega t)$ with water surrounding air. The plot shows an example of the growth of a perturbation after several periods of the drive as a function of drive amplitude b_1 and the number of wavelengths around the interface n.

For typical experimental values, [$b_0 = 290\ \mu$m, $f = 60$ Hz, $R(0) = 0.031$ m], with air as the inner fluid and water as the outer, the interface first becomes unstable at a drive amplitude of $b_1 = 9.6\ \mu$m at $n = 23$.

V. EXPERIMENTAL RESULTS

A. Onset of the instability

Several runs were made in the case of an incompressible fluid (water) surrounding a compressible fluid (air). The upper plate was driven sinusoidally and the movement measured with an attached accelerometer. Inner bubble radii ranged from 1 to 4 cm; the average plate gap b_0 from 230 to 420 μm; the frequency f from 30 to 90 Hz. Most runs were made with $b_0 = 290\ \mu$m, and $f = 60$ Hz.

When the plate is driven well below the threshold of the instability, the interface anneals to a circle, even if the interface starts off irregular or disconnected. As the amplitude of the drive is increased microscopic perturbations will grow and show up as barely visible waves that run along the interface. As the amplitude of the drive is further increased, another transition occurs, this one to large, stationary and highly irregularly shaped fingers.

Several figures are shown to illustrate the nature of the instability. For all, the inner fluid is air at $T = 20\,^\circ$C and the outer fluid is water with fluorescein dye. The initial gap is $b_0 = 290\ \mu$m. The radius of the initial, undriven interface $R = 0.03$ m. Figure 4 shows the small waves that appear on the interface as the amplitude of the drive is increased toward the predicted level for the instability. (These appear at $b_1 = 25\ \mu$m.) Figure 5 shows the growth of the highly irregular fingers at $b_1 = 30\ \mu$m as they convect around the interface.

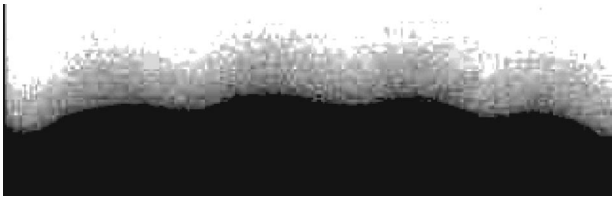

FIG. 4. The small traveling waves that appear on the interface before the growth of the larger, stationary fingers. The horizontal extent of the figure is about 5 mm, the wave amplitude about 0.3 mm.

The onset of these fingers is always convective—they do not appear simultaneously around the interface. The fingers can also be induced by a finite perturbation. That is, if the interface is being driven at an amplitude above the onset of the smaller waves (call this b_w), but below the level for the spontaneous growth of the fingers (call this b_f), the fingers can still be induced by perturbing the interface with an object placed between the plates and touched to the interface. Also, once the nonlinear waves are established, if b_1 is reduced to below b_f but remains above b_w, the fingers will persist indefinitely. Even as the driving amplitude is lowered further, the interface returns to circular by leaving fewer and fewer fingers, rather than by reducing the size of the fingers.

It is not clear which of these transitions corresponds to the instability predicted by the linear stability analysis. It is plausible that there exists an absolute instability at a value b_1 which is always higher than b_f, but is always masked by small, but finite, perturbations which induce the growth of the fingers and destroy the circular interface.

The interface is more stable than predicted by the linear stability analysis, with the waves and fingers appearing on the interface at values of the driving amplitude more than twice those predicted. Wetting effects, which are obviously important, but are not included in this linear stability analysis should work to stabilize the interface and increase the predicted driving amplitude of the onset of the instability closer to the observed values. The application of the velocity dependent wetting correction to the pressure jump at the interface of Park and Holmsy [9] to this problem is not straightforward. Their analysis gives the asymptotic correction for a finger travelling with constant velocity **v**.

Also, the assumption of a parabolic profile for **v** as a function of z may need to be modified. While using this

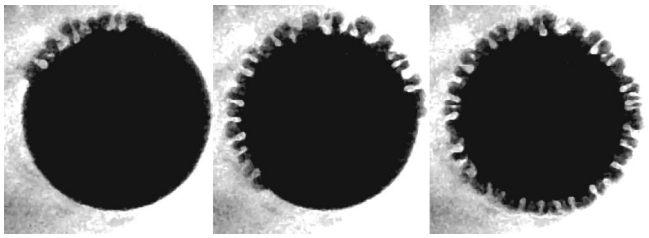

FIG. 5. Three images, 1/5 second apart—12 periods of the drive, showing the convection of the fully nonlinear fingers around the interface, just above the onset of the instability. The radius of the circle at this point in the drive is 0.032 m.

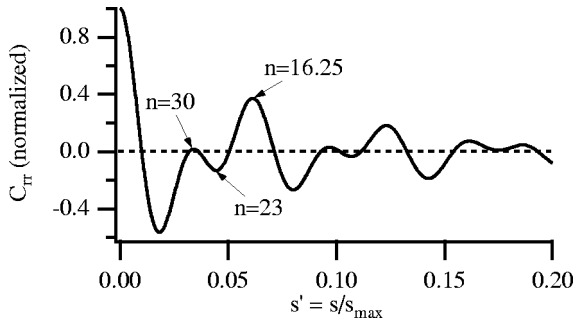

FIG. 6. The autocorrelation function of the radius of the interface as a function of scaled arc length, averaged for ten periods of the drive for the interface about 1 min after the images of Fig. 5.

profile gives good agreement with the experiment for the motion of the stable interface $R=R(t)$, the high velocities associated with the rapid motion of the unstable fingers may require its modification.

Understanding the wavelength selection of these fingers is problematic. First, the fingers very quickly grow away from a sinusoidal shape and nonlinear growth factors may then become important. Second, the highly distorted shape means that the interface position can no longer be characterized as a single-valued function of the angle.

In order to analyze the interface, the *x*-*y* interface data are transformed into radius r as a function of arc length s. The autocorrelation function C_{rr} of $r(s)$ is then examined. By creating a new scaled variable $s'=s/s_{\max}$ correlations functions from several frames of the video can be averaged.

C_{rr} for interfacial images just beyond the onset images of Fig. 5 has its first peak at a wavelength corresponding to $n=16.25$, with $n=23$ (the first unstable number of waves in the calculations) showing up as a strong minimum (peak to trough distance). Figure 6 shows the averaged correlation function for ten images about a minute after the onset of the fingers. The parameters of the current experimental apparatus cannot be varied sufficiently to test whether this correspondence in C_{rr} with the predicted first unstable wave number is coincidental or not.

B. Nonlinear fingers

Increasing the amplitude of the drive above b_f causes the fingers to break off the interface or to collide and introduce new bubbles into the dynamics. As b_1 is increased further disturbances on the interface grow larger, until the inner bubble itself is no longer stable. The inner fluid breaks into many smaller bubbles which eventually migrate out of the cell. (The dynamics of the bubbles are outside the realm of this paper.)

If the system is driven hard enough to sustain the fingers, but not hard enough to cause the fingers to collide or break off, one of the most curious features of the unstable interface can be seen. Viewing the interface at the same phase of the drive each time (at the point where the interface is the most extended), one can see that the interface has a memory and the fingers appear at the same location. They are not, however, always the same shape and size. Sometimes a finger will return to the same shape and size with each period of the drive, but sometimes it might alternate between two shapes. In fact, a stable period of two, four, six and eight oscillations have been observed, as well as fully chaotic oscillations.

Measuring the length of the fingers from the average position of the interface as a function of time, time series data for any finger can be obtained. Figure 7 shows portions of time series data for the lengths of two fingers for one run. Both fingers display chaotic oscillations, but during some time periods their length changes are clearly correlated, where during other times they are not. The fingers can be viewed as nonlinear oscillators which can display chaotic behavior, but are also clearly coupled to their surrounding fingers. Such systems of coupled chaotic oscillators are known to display synchronization [10]. This feature of fingers moving in and out of synchronization is a common feature whenever the interface has sustained fingers.

The *temporal* behavior of an individual finger is clearly connected to the spatial patterns in the interface nearby. Similar temporal patterns in the times series data of one finger are always seen to correlate to similar shapes. Figure 8 shows a closeup of a portion of the interface as that region undergoes period-four behavior.

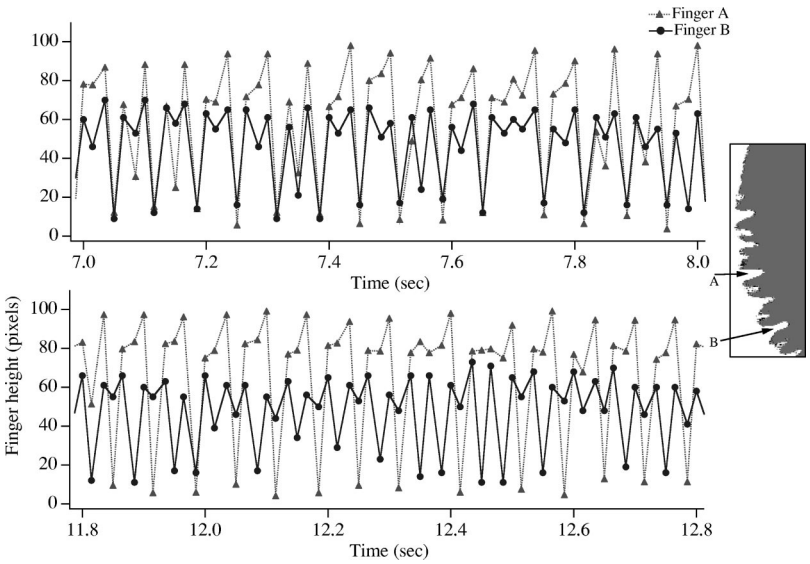

FIG. 7. Finger lengths vs time for two nearby fingers undergoing chaotic oscillations.

FIG. 8. Five images, each 1/60 s apart—one period of the drive—showing a portion of the driven interface undergoing period four behavior. The vertical extent of each image is approximately 1 cm.

VI. CONCLUSION

A modification of the Hele-Shaw cell in which the plate gap can be varied with time has been built. Appropriate modifications to the equation of motion and the continuity equation for fluids in such a cell were derived as were stability conditions for the interface between two fluids in the cell.

The experimental result for the case of an inner compressible fluid and an outer incompressible fluid show good agreement with the theoretical computations for the onset of the instability on the interface. As the interface is driven harder, highly nonlinear waves or fingers appear with several curious properties, including acting as coupled chaotic oscillators.

ACKNOWLEDGMENTS

The cell was originally built at the Naval Surface Warfare Center in White Oak, Maryland with Independent Research funds. This work was partially supported by Wheaton College through the Pew Great Lakes Science Cluster. The author wishes to thank Stephen Carrol, David Keller, and Laura Riihimaki for their valuable contributions.

[1] J. S. S. Hele-Shaw, Nature (London) **58**, 34 (1988).
[2] P. G. Saffman and G. I. Taylor, Proc. R. Soc. London, Ser. A **245**, 312 (1958).
[3] An excellent review of the computational and experimental work in Laplacian growth can be found in T. Viscek, *Fractal Growth Phenomena* (World Scientific, Singapore 1992).
[4] P. Tabeling and A. Libchaber, Phys. Rev. A **33**, 794 (1986).
[5] J. S. Langer, Rev. Mod. Phys. **52**, 1 (1980).
[6] D. Bensimon, L. P. Kadanoff, S. Liang, B. I. Shraiman, and L. Tang, Rev. Mod. Phys. **58**, 977 (1986).
[7] L. Paterson, J. Fluid Mech. **113**, 513 (1981).
[8] Etrema Products, Inc.
[9] C.-W. Park and G. M. Homsy, J. Fluid Mech. **139**, 291 (1984).
[10] L. Pecora and T. Carrol, Phys. Rev. Lett. **64**, 821 (1990).